THE JOURNAL OF BIOLOGICAL CHEMISTRY VOL. 292, NO. 3, pp. 925–935, January 20, 2017

Mineralocorticoid Receptor Deficiency in Macrophages Inhibits Atherosclerosis by Affecting Foam Cell Formation and Efferocytosis*

Received for publication, May 25, 2016, and in revised form, October 15, 2016 Published, JBC Papers in Press, November 23, 2016, DOI 10.1074/jbc.M116.739243

Zhu-Xia Shen (沈竹夏)[‡§¶], Xiao-Qing Chen (陈晓庆)[‖], Xue-Nan Sun (孙雪楠)[‡¶], Jian-Yong Sun (孙建永)[¶], Wu-Chang Zhang (张武昌)[‡], Xiao-Jun Zheng (郑晓君)[‡¶], Yu-Yao Zhang (张煜尧)[‡¶], Huan-Jing Shi (施焕敬)[¶], Jia-Wei Zhang (张嘉伟)[¶], Chao Li (李超)[‡¶], Jun Wang (王骏)[§], Xu Liu (刘旭)[‖], and Sheng-Zhong Duan (段胜仲)[‡1]

From the [‡]Laboratory of Oral Microbiology, Shanghai Research Institute of Stomatology, Shanghai Key Laboratory of Stomatology, Ninth People's Hospital, School of Stomatology, Shanghai Jiao Tong University School of Medicine, Shanghai 200011, China, the [§]Department of Cardiology, Jing'an District Centre Hospital of Shanghai, Huashan Hospital Jing'an Branch, Fudan University, Shanghai 200040, China, the [¶]Key Laboratory of Nutrition and Metabolism, Institute for Nutritional Sciences, Shanghai Institutes for Biological Sciences, Chinese Academy of Sciences, University of the Chinese Academy of Sciences, Shanghai 200031, China, and the [‖]Department of Cardiology, Shanghai Chest Hospital, Shanghai Jiao Tong University School of Medicine, Shanghai 200030, China

Edited by Dennis R. Voelker

Mineralocorticoid receptor (MR) has been considered as a potential target for treating atherosclerosis. However, the cellular and molecular mechanisms are not completely understood. We aim to explore the functions and mechanisms of macrophage MR in atherosclerosis. Atherosclerosis-susceptible LDLRKO chimeric mice with bone marrow cells from floxed control mice or from myeloid MR knock-out (MRKO) mice were generated and fed with high cholesterol diet. Oil red O staining showed that MRKO decreased atherosclerotic lesion area in LDLRKO mice. In another mouse model of atherosclerosis, MRKO/APOEKO mice and floxed control/APOEKO mice were generated and treated with angiotensin II. Similarly, MRKO inhibited the atherosclerotic lesion area in APOEKO mice. Histological analysis showed that MRKO increased collagen coverage and decreased necrosis and macrophage accumulation in the lesions. *In vitro* results demonstrated that MRKO suppressed macrophage foam cell formation and up-regulated the expression of genes involved in cholesterol efflux. Furthermore, MRKO decreased accumulation of apoptotic cells and increased effective efferocytosis in atherosclerotic lesions. *In vitro* study further revealed that MRKO increased the phagocytic index of macrophages without affecting their apoptosis. In conclusion, MRKO reduces high cholesterol- or angiotensin II-induced atherosclerosis and favorably changes plaque composition, likely improving plaque stability. Mechanistically, MR deficiency suppresses macrophage foam cell formation and up-regulates expression of genes related to cholesterol efflux, as well as increases effective efferocytosis and phagocytic capacity of macrophages.

Atherosclerosis is the underlying basis of coronary heart disease and cerebrovascular disease, which together account for nearly 80% of all deaths caused by cardiovascular diseases (1). Atherosclerotic cardiovascular diseases remain to be a leading cause of mortality and morbidity worldwide, posing a great threat to public health (2). New strategies and new targets are in need to treat atherosclerosis more effectively.

Macrophages are the major immune cells in atherosclerotic plaques and play essential roles during the whole process of atherosclerosis in different aspects, including inflammation, foam cell formation, necrosis, and phagocytic clearance (3, 4). In the early stages, macrophages accumulated in the subendothelial space ingest modified lipids to become foam cells that are a hallmark of atherosclerosis and the major component of early fatty streak lesions (5). These macrophage-derived foam cells secrete inflammatory cytokines and chemokines to amplify inflammatory response and to induce more accumulation of macrophages/foam cells, propelling expansion and progression of atherosclerotic plaques. In advanced lesions, apoptosis of macrophages/foam cells rapidly increases, whereas the ability of neighboring macrophages/foam cells to effectively clear the apoptotic cells (effective efferocytosis) decreases, both of which contribute to plaque necrosis and elevated inflammation. Therefore, targeting macrophages specifically has emerged as a promising novel strategy to combat atherosclerosis (3).

Recent studies have illustrated that mineralocorticoid receptor (MR)[2] is a critical control point of macrophage functions and may play pivotal roles in atherogenesis. MR is a classical nuclear receptor, and its functions in the cardiovascular system have been extensively studied (6–8). MR antagonists (spirono-

* This work was supported by National Natural Science Foundation of China Grants 31671181, 31400987, 91339110, and 31371153; Science and Technology Commission of Shanghai Municipality Grant 15140904400; and the Shanghai Summit & Plateau Discipline Developing Projects. The authors declare that they have no conflicts of interest with the contents of this article.

[1] To whom correspondence should be addressed: Ninth People's Hospital, Shanghai Jiao Tong University School of Medicine, 639 Zhizaoju Rd., Shanghai 200011, China. Tel.: 86-21-23271699, Ext. 5962; Fax: 86-21-63136856; E-mail: duansz@shsmu.edu.cn.

[2] The abbreviations used are: MR, mineralocorticoid receptor; FC, floxed control; MRKO, myeloid MR knock-out; LDLRKO, LDLR knock-out; Apo, apolipoprotein; APOEKO, ApoE knock-out; PPARγ, peroxisome proliferator-activated receptorγ; LXR, liver X receptor; ABCG1, ATP-binding cassette transporter G1; 7KC, 7-ketocholesterol; AngII, angiotensin II; BMDM, bone marrow-derived macrophage; qPCR, quantitative PCR; oxLDL, oxidized low-density lipoprotein.

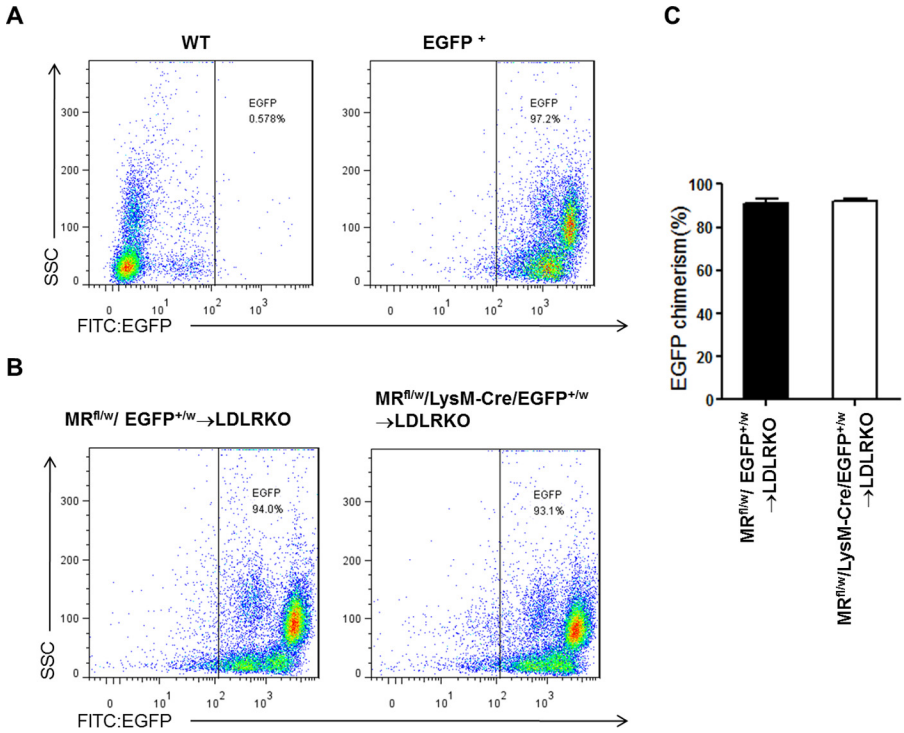

FIGURE 1. **Flow cytometric analysis of chimeric percentages 4 weeks after bone marrow transplantation.** *A*, representative results of peripheral blood preparation from WT mice (negative control) and EGFP$^+$ transgenic mice (positive control). *B*, representative results of peripheral blood preparation from chimeric mice (MR$^{fl/w}$/EGFP$^{+/w}$ → LDLRKO mice or MR$^{fl/w}$/LysM-Cre/EGFP$^{+/w}$ → LDLRKO mice). *C*, quantification of chimeric percentage of the chimeric mice.

lactone and eplerenone) are highly effective in treating heart failure (9–11). Animal studies have shown that these antagonists inhibit atherosclerosis, whereas aldosterone, an endogenous agonist of MR, promotes atherosclerosis (8, 12). Utilizing a myeloid MR knock-out (MRKO) mouse model, we and others have previously demonstrated that MR regulates macrophage polarization and inflammation and that macrophage MR is important in controlling cardiac and vascular remodeling (13–17). However, it has remained unknown whether macrophage MR plays a role in atherosclerosis.

In the current study, we aim to study the function of macrophage MR in atherosclerosis and explore the mechanisms. We first use both low density lipoprotein receptor knock-out (LDLRKO) mice and apolipoprotein E knock-out (APOEKO) mice as the atherogenic mouse models, in combination with MRKO mice, to investigate whether macrophage MR affects atherogenesis. Then we further explore the possible mechanisms by analyzing the impacts of MR deficiency on foam cell formation and effective efferocytosis.

Results

Myeloid MR Deficiency Suppresses High Cholesterol-induced Atherosclerosis in LDLRKO Mice—To study whether myeloid MR deficiency contributes to atherogenesis, we performed bone marrow transplantation to generate atherosclerosis-susceptible LDLRKO chimeric mice with FC (FC → LDLRKO) or MRKO bone marrow cells (MRKO → LDLRKO). Four weeks after bone marrow transplantation, the chimeric percentage was more than 90% (Fig. 1). After feeding with a Western diet (high cholesterol) for 16 weeks, development of atherosclerosis was analyzed. Oil red O staining of the entire aorta demonstrated that the area of atherosclerotic lesions was significantly decreased in MRKO → LDLRKO mice compared with FC → LDLRKO mice (47.1% decrease; Fig. 2, *A* and *B*). Similarly, oil

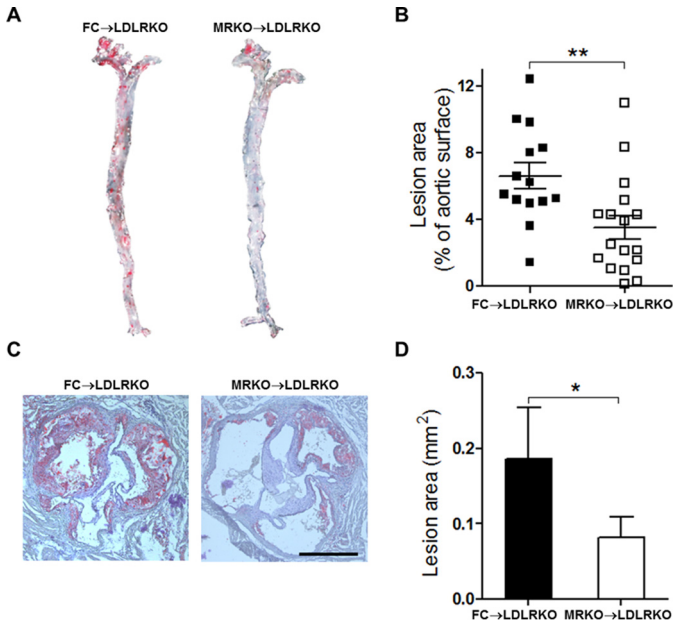

FIGURE 2. **Myeloid MR deficiency suppresses atherosclerosis in LDLRKO mice.** *A*, representative images of en face oil red O staining of aortas from LDLRKO mice transplanted with FC bone marrow (FC → LDLRKO) or MRKO bone marrow (MRKO → LDLRKO) and fed with a Western diet for 16 weeks. The atherosclerotic lesion areas stained *red*. *B*, quantification of *A* as percentage of total aortic surface (n = 14–17; male, n = 7:9; female, n = 7:8). *C*, representative images of oil red O staining of the aortic sinus from FC → LDLRKO mice and MRKO → LDLRKO mice. *Scale bar*, 500 μm. *D*, quantification of the atherosclerotic lesion area of the aortic sinus (n = 9–10). *, $p < 0.05$; **, $p < 0.01$.

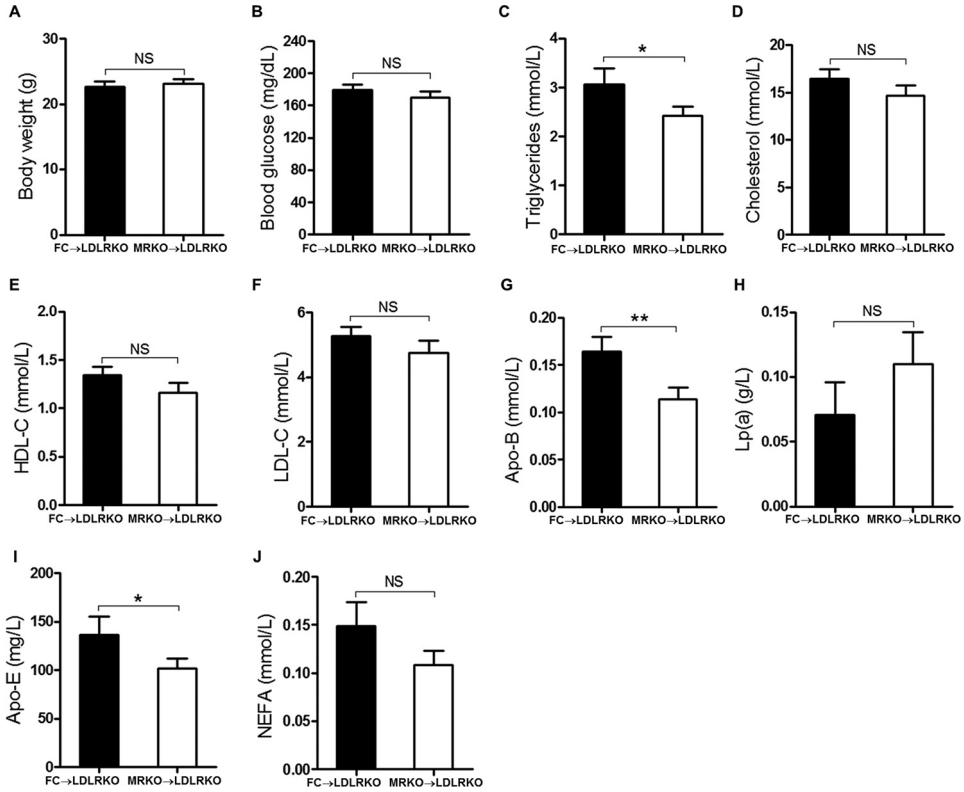

FIGURE 3. **Effects of myeloid MR deficiency on metabolic parameters of LDLRKO mice.** FC → LDLRKO mice and MRKO → LDLRKO mice were fed with a Western diet for 16 weeks. *A*, body weight. *B*, blood glucose. *C*, plasma triglycerides levels. *D*, plasma cholesterol levels. *E*, high density lipoprotein cholesterol. *F*, low density lipoprotein cholesterol. *G*, apolipoprotein B. *H*, lipoprotein a (*LP(a)*). *I*, apolipoprotein E. *J*, non-esterified fatty acids (NEFA). $n = 14–17$ for all panels. *NS*, not significant. *, $p < 0.05$; **, $p < 0.01$.

red O staining of cross-sections of aortic sinus revealed significantly smaller lesion areas in the aortic sinus in MRKO → LDLRKO mice (Fig. 2, *C* and *D*). Most metabolic parameters were undistinguishable between the two groups, except that triglycerides, apolipoprotein (Apo)B and ApoE were decreased in MRKO → LDLRKO mice (Fig. 3).

Myeloid MR Deficiency Suppresses Angiotensin II-induced Atherosclerosis in APOEKO Mice—Furthermore, we studied the function of myeloid MR in angiotensin II-induced atherosclerosis. MRKO/APOEKO (double knock-out) mice and FC/APOEKO mice were generated and treated with AngII or saline (control). MRKO/APOEKO mice showed a significant decrease (35%) in atherosclerotic lesions when treated with saline (Fig. 4, *A* and *B*). MRKO/APOEKO mice also showed a significant decrease (47.7%) in atherosclerotic lesions with AngII by en face staining of the aorta (Fig. 4, *C* and *D*). Oil red O staining of cross-sections of aortic sinus also showed significantly smaller lesion areas in the aortic sinus in MRKO/APOEKO mice with AngII (Fig. 4, *E* and *F*). MRKO did not affect the development of abdominal aortic aneurysm in this model (Fig. 4, *G–I*). Metabolic parameters were comparable between MRKO/APOEKO mice and FC/APOEKO mice (Fig. 5). Thus, myeloid MR deficiency suppresses AngII-induced atherosclerosis in atherogenic mice without changing the metabolic parameters, indicating direct influence of MRKO myeloid cells, particularly macrophages.

Myeloid MR Deficiency Affects Plaque Composition in LDLRKO Mice—We next analyzed components of atherosclerotic plaques by histological staining and immunofluorescence. Collagen accumulation, necrosis, and inflammation are important features that could affect atherosclerotic plaque stability. Interestingly, picrosirius red staining demonstrated that myeloid MR deficiency significantly increased the ratio of plaque collagen coverage to total lesion area at the aortic sinus level (66.1% increase; Fig. 6, *A* and *B*). Further, hematoxylin and eosin staining of the aortic sinus showed that myeloid MR deficiency decreased necrotic area (57.0% reduction; Fig. 6, *C* and *D*). At cellular level, the amounts of macrophages in plaques closely correlate with atherosclerotic lesion formation and plaque stability (18). Immunofluorescence staining of macrophages (mac2) showed that macrophage accumulation in atherosclerotic lesions was significantly decreased in MRKO → LDLRKO mice compared with FC → LDLRKO mice (49.1% reduction; Fig. 6, *E* and *F*). Negative control (replacing mac2 antibody with IgG) did not have any positive staining for macrophages (Fig. 6*G*). Together, these changes in MRKO → LDLRKO mice suggest that myeloid MR deficiency may improve the stability of atherosclerotic plaques.

Myeloid MR Deficiency Inhibits Foam Cell Formation and Up-regulates Expression of Genes Related to Cholesterol Efflux—Accumulation of macrophages in lesions and subsequent foam cell formation by cholesterol accumulation is a critical early step in the pathogenesis of atherosclerosis(4). We tested whether myeloid MR deficiency affected foam cell formation. First, bone marrow-derived macrophages (BMDMs) were obtained from FC → LDLRKO mice and MRKO → LDLRKO mice after feeding with a Western diet. Oil red O staining revealed that foam cell formation markedly decreased in

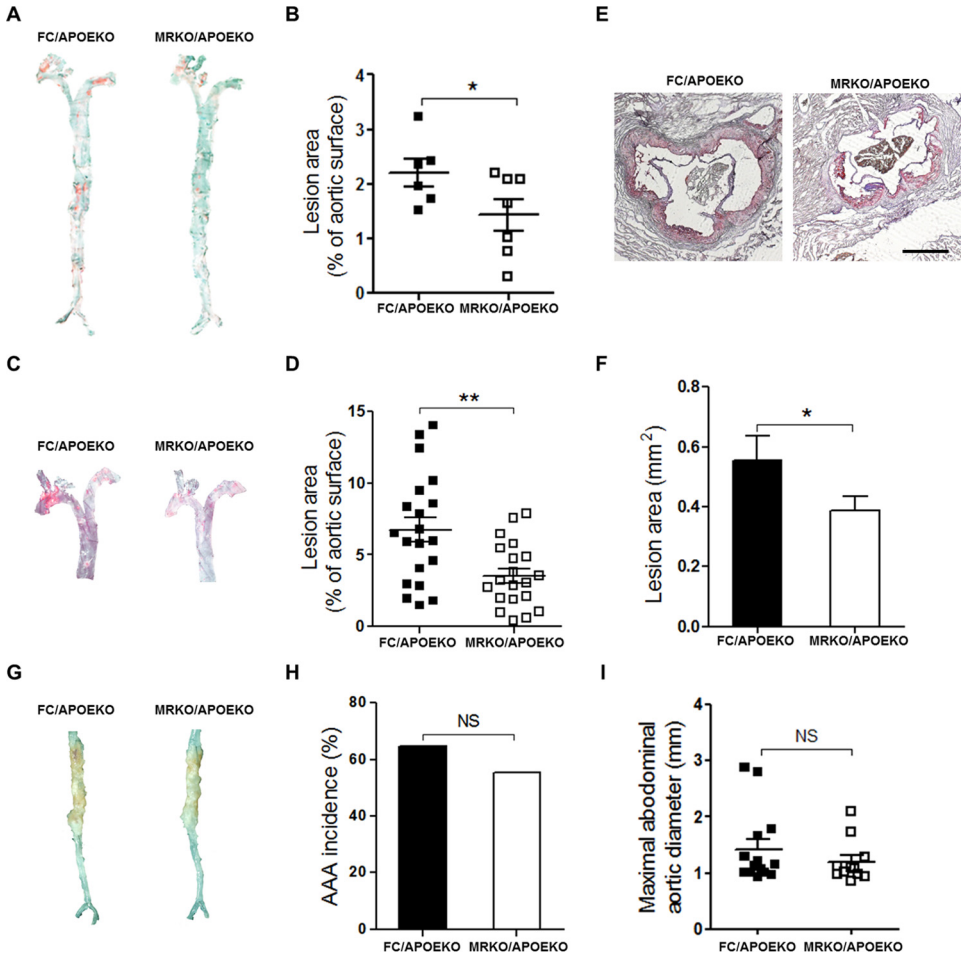

FIGURE 4. **Effects of myeloid MR deficiency on atherosclerosis and abdominal aortic aneurysm in APOEKO mice.** *A*, representative images of en face oil red O staining of aortas from FC/APOEKO mice and MRKO/APOEKO mice infused with saline for 28 days. *B*, quantification of *A* as percentage of total aortic surface ($n = 6–7$). *C*, representative images of en face oil red O staining of aortas from FC/APOEKO mice and MRKO/APOEKO mice infused with AngII for 28 days. *D*, quantification of *C* as percentage of total aortic surface (male, $n = 6–8$; female, $n = 14–12$). *E*, representative images of oil red O staining of the aortic sinus from FC/APOEKO mice and MRKO/APOEKO mice. *Scale bar*, 500 μm. *F*, quantification of the atherosclerotic lesion area of the aortic sinus ($n = 5$). *G*, representative images of aortic aneurysm in abdominal aortas from FC/APOEKO mice and MRKO/APOEKO mice infused with AngII for 28 days. *H*, the incidence of abdominal aortic aneurysm in FC/APOEKO and MRKO/APOEKO mice ($n = 16–17$). *I*, maximal aortic diameter of abdominal aortas from FC/APOEKO and MRKO/APOEKO mice ($n = 11–14$). *NS*, not significant. *, $p < 0.05$; **, $p < 0.01$.

BMDMs of MRKO → LDLRKO mice compared with those of FC → LDLRKO mice (Fig. 7, *A* and *B*). Then we examined the impact of myeloid MR deficiency on expression of genes involved in cholesterol balance in these cells. Using qPCR, we assessed mRNA levels of peroxisome proliferator-activated receptor-γ (PPARγ), liver X receptor-α (LXRα), LXRβ, retinoid X receptor α, ATP-binding cassette transporter subfamily A1 (ABCA1), and ABCG1. The results showed that myeloid MR deficiency up-regulated gene expression of PPARγ, LXRα, retinoid X receptor α, and ABCG1 (Fig. 7*C*). Expression of genes such as scavenger receptor A, scavenger receptor BI, CD36, CD68, and lectin-like oxLDL receptor-1, was not significantly altered by MRKO, indicating that uptake of oxLDL was not affected (Fig. 7*C*). As expected, gene expression of MR was markedly suppressed in BMDMs from mice transplanted with MRKO bone marrow (Fig. 7*C*). Second, after incubation with oxLDL, peritoneal macrophages from MRKO/APOEKO mice developed much less foam cells than those from FC/APOEKO mice (Fig. 7, *D* and *E*). qPCR results showed that myeloid MR deficiency up-regulated gene expression of PPARγ, LXRα, and ABCG1 in these cells (Fig. 7*F*). Similarly, expression of genes related to uptake of oxLDL was not affected by MRKO (Fig. 7*F*). Third, flow cytometric analysis showed that peritoneal macrophages from MRKO/APOEKO mice engulfed less DiI-oxLDL than those from FC/APOEKO mice (Fig. 7, *G* and *H*). Fourth, foam cell formation decreased in peritoneal macrophages of MRKO mice compared with those of FC mice *in vitro* (Fig. 7, *I* and *J*). In addition, our results showed that MR deficiency did not influence oxidative status of macrophages (Fig. 8).

Myeloid MR Deficiency Increases Effective Efferocytosis of Macrophages—Macrophage efferocytosis plays essential roles in lesion development. We investigated whether myeloid MR deficiency affected macrophages efferocytosis (efficiency of phagocytic clearance of apoptotic cells). To test efferocytosis *in vivo*, we first detected apoptotic cells in the atherosclerotic plaques of FC → LDLRKO mice and MRKO → LDLRKO mice by the TUNEL staining. We found that myeloid MR deficiency significantly decreased the number of apoptotic cells in lesions (Fig. 9, *A* and *B*), indicating the possibility of increased effective efferocytosis. Indeed, the atherosclerotic plaques of MRKO →

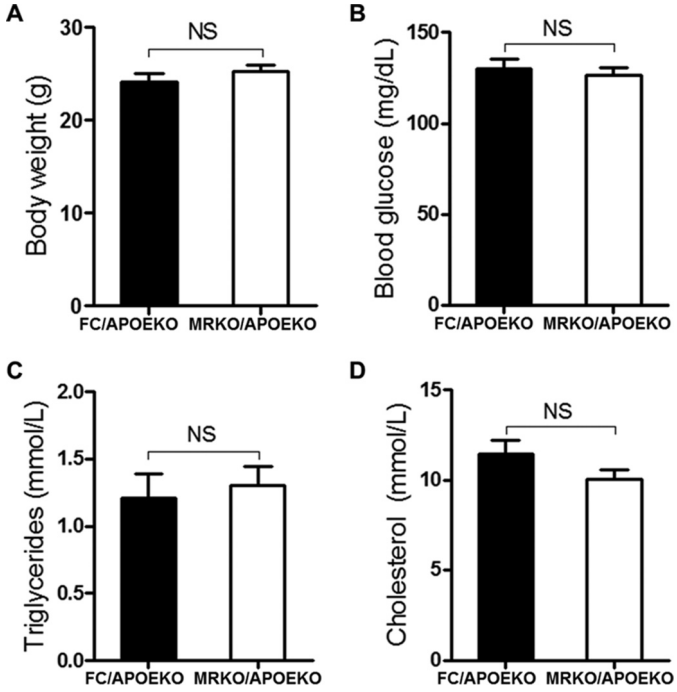

FIGURE 5. **Effects of myeloid MR deficiency on metabolic parameters of APOEKO mice.** MRKO/APOEKO mice and FC/APOEKO mice were treated with AngII for 4 weeks. *A*, body weight. *B*, blood glucose. *C*, plasma triglycerides levels. *D*, plasma cholesterol levels. $n = 12–13$ for all panels. *NS*, not significant.

LDLRKO mice had a higher efferocytosis index (the ratio of macrophage-associated to free apoptotic cells) than those of FC → LDLRKO mice (Fig. 9, *A* and *C*). Therefore, myeloid MR deficiency increased macrophage efferocytosis in the atherosclerotic lesions. Macrophages from FC and MRKO mice were used to further test the impacts of MR deficiency on the phagocytic ability of macrophages. Staining of F4/80 and calcein AM almost completely merged, suggesting that most viable cells were phagocytic macrophages (Fig. 9*D*). Further merge with staining of annexin V demonstrated that macrophages (as phagocytes) from MRKO mice phagocytized much more apoptotic cells than those from FC mice (Fig. 9*D*) and that both BMDMs and peritoneal macrophages from MRKO mice had higher phagocytic index (Fig. 9, *E* and *F*). MR deficiency did not affect apoptosis of macrophages (Fig. 9, *G* and *H*), further supporting the possibility that the observed decrease of apoptotic cells in atherosclerotic lesions was most likely attributable to increased effective efferocytosis.

Discussion

Although it has been demonstrated that antagonists of MR suppress atherosclerosis in different animal models (19–22), the cell type-specific effects of MR has not been well delineated. Our results showed that MR deficiency in macrophages attenuated atherosclerotic plaques in both high cholesterol diet-fed LRLRKO mice and AngII-infused APOEKO mice. MRKO increased collagen content but decreased necrosis and macrophage content in the plaques. Mechanistically, MRKO mitigated foam cell formation and up-regulated effective efferocytosis.

Our data suggested that targeting macrophage MR specifically might be a feasible strategy to treat atherosclerosis. Our results revealed that MR blockade in macrophages was sufficient to mitigate atherosclerosis and likely improve plaque vulnerability, indicating that macrophage MR plays essential roles in the process of atherogenesis. It is plausible to treat atherosclerosis by selectively blockade of MR in macrophages using nanoparticles, which have been proved to be effective as delivery vehicles in the setting of atherosclerosis (3, 23–26). This strategy allows local delivery of agents to block macrophage MR in atherosclerotic lesions, likely improving efficacy and circumventing systemic side effects.

Our results indicated that macrophage MR deficiency improved stability of atherosclerotic plaques. First, MRKO increased collagen coverage of atherosclerotic plaques. The amount of collagen is a major determinant for the thickness of fibrous cap that significantly affects plaque stability (27). Second, MRKO improved effective efferocytosis and decreased macrophage accumulation and necrosis in atherosclerotic plaques. Apoptosis of macrophages and defective efferocytosis led to necrosis (4), another risk factor for plaque instability (27). Our results suggested that MRKO mainly improved efferocytosis that might lead to suppressed macrophage accumulation and necrosis.

Macrophage MR deficiency inhibited foam cell formation likely by up-regulating expression of genes related to cholesterol efflux. Although it had been shown that antagonists of MR suppress the abilities of macrophages to oxidize LDL and uptake oxLDL (21, 28), it was not clear whether MR directly affects foam cell formation. Our results demonstrated that MR deficiency in macrophages inhibited foam cell formation, illustrating a direct role for macrophage MR. Macrophage reverse cholesterol transport plays central roles in the process of foam cell formation. MRKO increased expression of genes involved in reverse cholesterol transport. PPARγ and LXRα are among the most critical regulators of macrophage reverse cholesterol transport. The importance of both LXRα-ABCA1 and PPARγ-ABCG1 axis has been established in promoting cholesterol efflux and suppressing macrophage foam cell formation (29, 30). PPARγ also directly regulates LXRα, and a PPARγ-LXR-ABCA1 pathway has been proposed (30, 31). Our results showed that ABCG1, but not ABCA1, was affected by MRKO in macrophages. Given that both ABCG1 and ABCA1 are target genes of LXRα, a PPARγ-LXRα-ABCG1 axis may well exist in macrophages to mediate the influence of MR deficiency on cholesterol efflux and foam cell formation. However, it remains to be further interrogated whether macrophage MR exerts its effects by directly acting on the PPARγ-LXRα-ABCG1 axis. It is also worthwhile to mention that MR deficiency does not significantly affect the expression of PPARγ in macrophages at baseline (14). Our current data showed significant up-regulation of PPARγ in MRKO macrophages incubated with oxLDL, suggesting that pro-atherogenic factors may be required for the effect.

MR deficiency in macrophages increased effective efferocytosis through up-regulating phagocytic capacity. Defective macrophages efferocytosis is typical in advanced atherosclerosis and an underlying mechanism for necrosis and rupture of

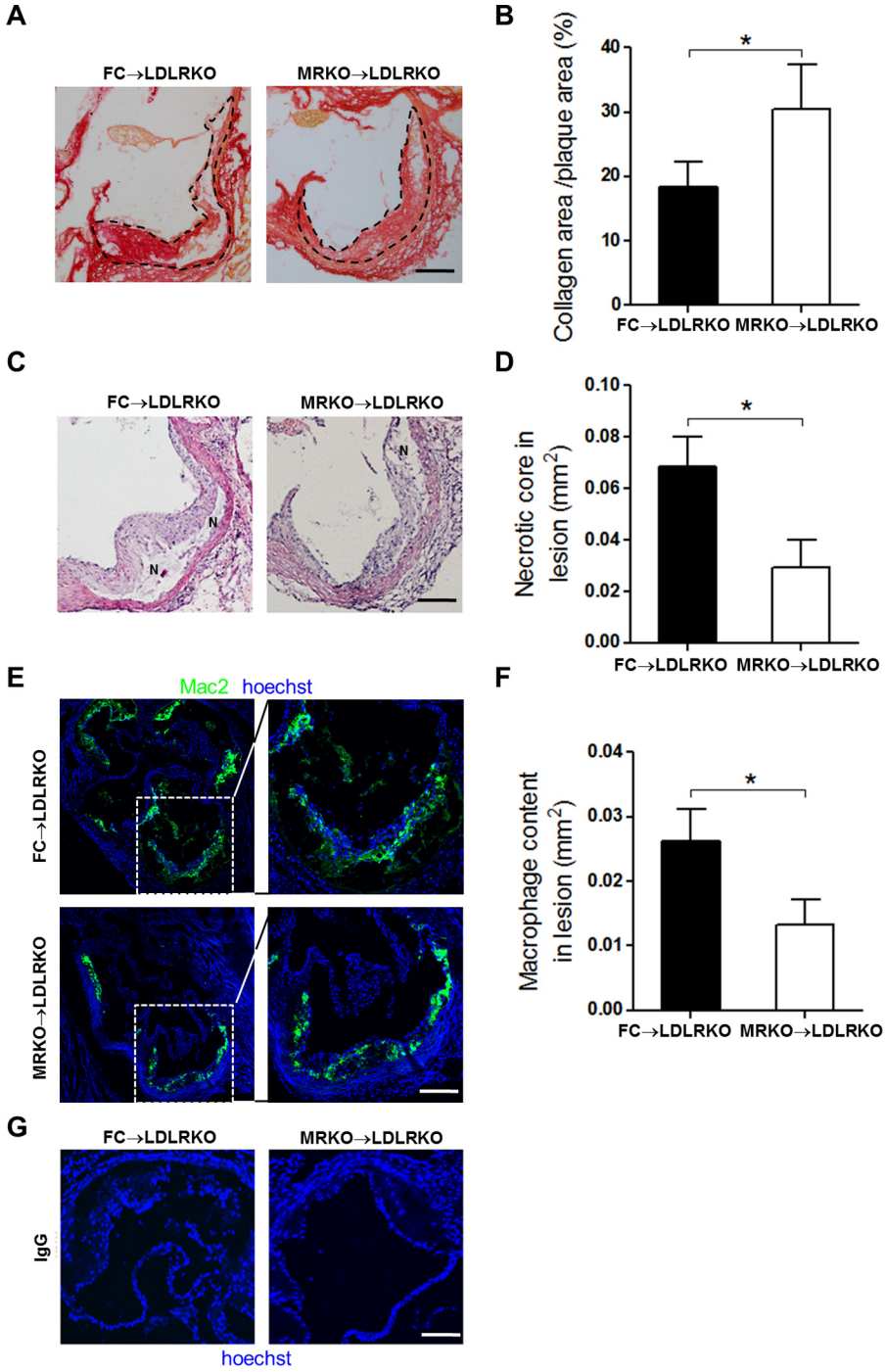

FIGURE 6. **Effects of myeloid MR deficiency on plaque composition.** *A*, representative images of picrosirius red staining for collagen of the aortic sinus from FC → LDLRKO mice and MRKO → LDLRKO mice fed with a Western diet for 16 weeks. The collagen areas were stained *red*. Atherosclerotic plaques are outlined by *black dotted lines*. *B*, quantification of the ratio of collagen coverage to total plaque area ($n = 6–7$). *C*, representative images of hematoxylin and eosin (*H&E*) staining of the aortic sinus. *N*, necrotic core. *D*, quantification of the necrotic area at aortic sinus level ($n = 7–9$). *E*, representative immunofluorescence staining of mac2 to detect macrophages/foam cells in aortic sinus of FC → LDLRKO mice and MRKO → LDLRKO mice. *F*, quantification of macrophage content within the aortic sinus region ($n = 5–8$). *G*, immunofluorescence staining of aortic cross sections using IgG as the primary antibody (negative control). *Scale bars*, 100 μm. *, $p < 0.05$.

atherosclerotic plaques (5, 32). Our results showed that MRKO improved macrophage efferocytosis both *in vivo* and *in vitro*. Furthermore, MRKO increased the phagocytic index without affecting apoptosis of macrophages, suggesting that phagocytic capacity was the major contributor.

Taken altogether, our data have revealed the important roles of macrophage MR in foam cell formation, efferocytosis, and high cholesterol- or AngII-induced atherosclerosis. The study supports targeting macrophage MR as a potential strategy to treat atherosclerosis.

Experimental Procedures

Animal Procedures—Myeloid MR knock-out (MRKO: $MR^{fl/fl}$, LysM-Cre) and floxed control (FC: $MR^{fl/fl}$) mice were gener-

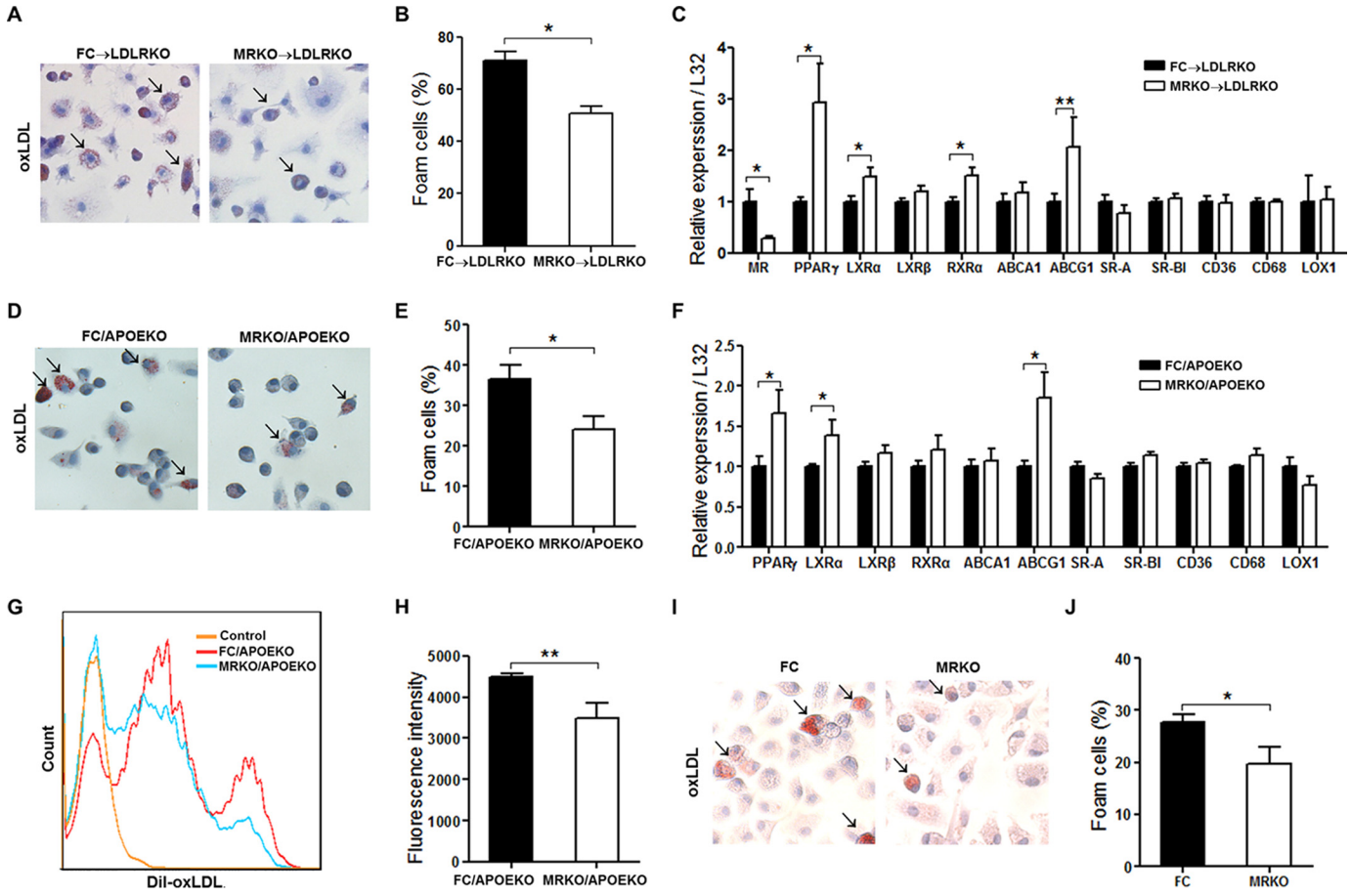

FIGURE 7. **Myeloid MR deficiency decreases foam cell formation.** *A*, representative oil red O staining of foam cell formation *ex vivo*. BMDMs were isolated from Western diet-fed FC → LDLRKO or MRKO → LDLRKO mice and incubated with 50 μg/ml oxLDL for 20 h. *Arrows* point to positively stained cells. *B*, quantification of foam cell formation ($n = 7$). *C*, expression of genes related to cholesterol homeostasis in BMDMs incubated with 50 μg/ml oxLDL for 20 h ($n = 7$). RT-qPCR was used to measure the relative gene expression level. L32 was used as an endogenous control. *D*, representative oil red O staining of peritoneal macrophages from MRKO/APOEKO mice and FC/APOEKO mice incubated with 50 μg/ml oxLDL for 48 h. *Arrows* point to positively stained cells. *E*, quantification of peritoneal macrophage foam cell formation *in vitro* ($n = 5$). *F*, expression of genes related to cholesterol homeostasis in peritoneal macrophages incubated with 50 μg/ml oxLDL for 48 h ($n = 5$). *G*, representative flow cytometric analysis of peritoneal macrophages incubated with 5 μg/ml DiI-oxLDL for 12 h. *H*, quantification of the results of flow cytometric analysis ($n = 4$). *I*, representative oil red O staining of peritoneal macrophages from MRKO mice and FC mice incubated with 50 μg/ml oxLDL for 48 h. *Arrows* point to positively stained cells. *J*, quantification of *I* as foam cell formation ($n = 3$). *, $p < 0.05$; **, $p < 0.01$.

ated as previously described (14). MRKO/APOEKO mice were created by crossing MRKO and APOEKO mice to yield double heterozygotes that were further crossed to produce double knock-out homozygotes (MRKO/APOEKO: $MR^{fl/fl}$, LysM-Cre, $APOE^{-/-}$) and control (FC/APOEKO: $MR^{fl/fl}$, $APOE^{-/-}$) mice. Sex- and age-matched littermates were used for experiments. All animal protocols were approved by the Institutional Review and Ethics Board of Ninth People's Hospital, Shanghai Jiao Tong University School of Medicine and the Institutional Animal Care and Use Committee of Institute for Nutritional Sciences, Shanghai Institutes for Biological Sciences, Chinese Academy of Sciences.

Bone Marrow Transplantation—6–8-week-old male or female recipient LDLRKO mice were irradiated with 900 rads (Gamma Cell 3000Elan, Nordian, Canada). Bone marrow cells from donor mice (MRKO or FC mice) were collected and at least 5×10^6 bone marrow cells were injected into each recipient mouse intravenously. Mice without bone marrow transplantation all died in 1–2 weeks after irradiation, and the survival rate of mice with FC or MRKO bone marrow cells was ~90% (Table 1). After reconstitution for 4 weeks, the mice were fed with a Western diet containing 1.25% cholesterol (Research diet, D12108C) for 16 weeks (33).

To evaluate chimeric percentage, MRKO mice were bred to EGFP mice to yield double heterozygotes ($MR^{fl/w}$/LysM-Cre/$EGFP^{+/w}$ or $MR^{fl/w}$/$EGFP^{+/w}$). Bone marrow cells of these mice were injected into recipient LDLRKO mouse after irradiation. After 28 days, blood of chimeric mice ($MR^{fl/w}$/LysM-Cre/$EGFP^{+/w}$ → LDLRKO or $MR^{fl/w}$/$EGFP^{+/w}$ → LDLRKO) were analyzed by flow cytometry to evaluate the percentage of EGFP chimerism.

Infusion of AngII—Alzet osmotic minipumps (model 2004; Alzert) were implanted into male or female MRKO/APOEKO and FC/APOEKO mice at 6 months of age. After the mice were anesthetized by isoflurane inhaling, minipumps were placed into the subcutaneous space of mice through a small incision in the back of the neck. The incision was then sutured. The osmotic minipumps delivered AngII (Sigma) at 1.44 mg/kg/day for 4 weeks. AngII was dissolved in sterile saline, and osmotic minipumps delivering saline were used as controls (34).

Atherosclerotic Lesion Analysis—The mice were euthanized by anesthetic overdose, and the aortas were dissected. For en

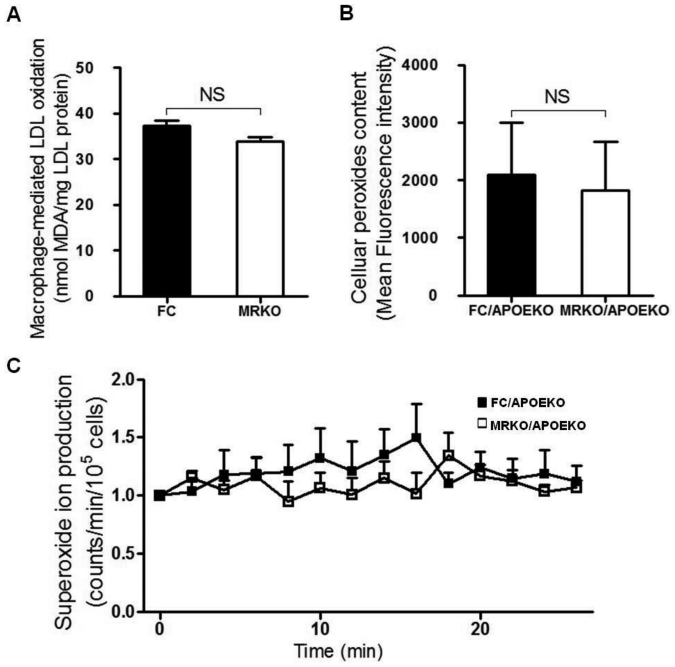

FIGURE 8. **Myeloid MR deficiency does not affect oxidative status of macrophages.** *A*, macrophage-mediated LDL oxidation (n = 7–8). *MDA*, malondialyde. *B*, lipid peroxide content (n = 6–7). *C*, lucigenin-derived superoxide ion production in macrophages (n = 4–5). *NS*, not significant.

face analysis, the aortas were washed for 2–3 min in 70% alcohol, stained in Sudan IV for 6 min, washed in 80% alcohol for 6 min, and then washed three times in PBS. Finally, the stained aortas were pinned flat, intimal side up, onto plain black wax for analysis. Lesion development was expressed as percentage of lesion areas (red staining) to total aortic surface area. In addition, aortic roots were fixed in 4% paraformaldehyde in PBS overnight at 4 °C, frozen in OCT medium, and cut into sections (10 μm) using a cryostat. Sections were dried at room temperature, incubated in 60% isopropanol for 10 min, stained in oil red O solution for 5 min, washed in 60% isopropanol for 30 s, and then counterstained with hematoxylin. Lesion area was evaluated using Adobe Photoshop and Image-Pro Plus software (35).

Analysis of Abdominal Aortic Aneurysm—The mice were euthanized by anesthetic overdose, and the aortas were dissected. The aortas were fixed in 4% paraformaldehyde in PBS overnight at 4 °C. Photographs were taken under microscope and further analyzed.

Lipids Analysis—Blood samples were collected from mice using EDTA as anticoagulant. The samples were centrifuged at 3000 rpm for 15 min to obtain plasma that was used for determination of cholesterol and triglycerides concentration (35).

Histologic Analysis—Frozen sections of aortic roots were stained with picrosirius red to assess collagen content of the plaques (36). In addition, hemotoxylin and eosin staining was used to determine necrotic areas.

Immunofluorescence Staining—Frozen sections of aortic roots were fixed in acetone for 10 min, rehydrated with PBS, incubated in blocking buffer containing normal goat serum, stained with primary antibody overnight, and then stained with secondary antibody. Hoechst was used to identify nuclei (37). Macrophages in plaques were detected using mac2 primary antibody. Apoptotic cells in plaques were detected using TUNEL kit (Roche). The results were analyzed using an Olympus inverted fluorescent confocal microscope.

Bone Marrow-derived Macrophages—BMDMs were obtained as described before (38). Briefly, after the mice were euthanized by anesthetic overdose, bone marrow cells were obtained from hind legs. The cells were plated in RPMI 1640 containing 20% FBS and 30% L929-cell conditioned medium for 7 days before use.

Thioglycollate-elicited Peritoneal Macrophages—Thioglycollate-elicited peritoneal macrophages were obtained as described before (39). Briefly, 1 ml of 3% Brewer's thioglycollate medium (Sigma) per mouse were injected into the peritoneal cavity. After 4 days, the mice were euthanized with anesthetic overdose. Peritoneal exudate cells were obtained by rinsing the peritoneal cavity with 5 ml of cold PBS three times, centrifuged at 1000 rpm for 10 min, and plated in culture media (DMEM containing 10% FBS). After 2 h, the cells were washed with PBS, and new culture medium was added.

Analysis of Foam Cell Formation—Peritoneal macrophages or BMDMs were plated in DMEM or RPMI 1640 containing FBS and different concentration of oxLDL. The cells were fixed for 30 min in 10% formalin, rinsed in double distilled H_2O, washed in 60% isopropanol for 5 min, stained in Oil Red O solution for 5 min, and then counterstained with hematoxylin for 1 min. The percentage of foam cells were expressed as percentages of oil red O-positive cells to total macrophages (40). Additionally, peritoneal macrophages were incubated with DiI-oxLDL for 12 h, and the fluorescent signals were analyzed by flow cytometry.

Analysis of Gene Expression—Total RNA was isolated from cells and converted into cDNA using a PrimeScript reverse transcriptase reagent kit (Takara). RT-qPCR was carried out using SYBER green master mixes and custom primers on an ABI7900 real time PCR machine (Life Technologies). Relative gene expression was analyzed using the ΔΔCt method with L32 as a normalizing standard.

Flow Cytometric Analysis—Tail vein blood of chimeric mice was collected in capillary tubes with anticoagulant. After lysis of red blood cells, blood samples were analyzed by flow cytometer (FACSAria; BD Biosciences) to evaluate the fluorescent signals of EGFP. For analysis of foam cell formation, DiI-oxLDL-treated peritoneal macrophages were detached with trypsin. Samples were subsequently analyzed by flow cytometer (excitation, 514 nm; emission, 565 nm). Mean fluorescence intensity was quantified using FlowJo software (BD Biosciences).

Determination of Macrophage Phagocytic Ability—To assess macrophage efferocytosis in atherosclerotic lesions, sections of aortic roots were stained with mac2 to detect macrophages, with TUNEL to detect apoptotic cells, and with DAPI to detect nuclei. Apoptotic nuclei that overlapped with macrophages were considered "macrophage-associated," and those that did not overlap with macrophages were considered "free." The ratio of macrophage-associated apoptotic cells to free apoptotic cells was calculated as the efferocytosis index (41). For *in vitro* assays, macrophages (peritoneal macrophages or BMDMs) were rendered apoptotic by treatment with 15 μg/ml 7-keto-

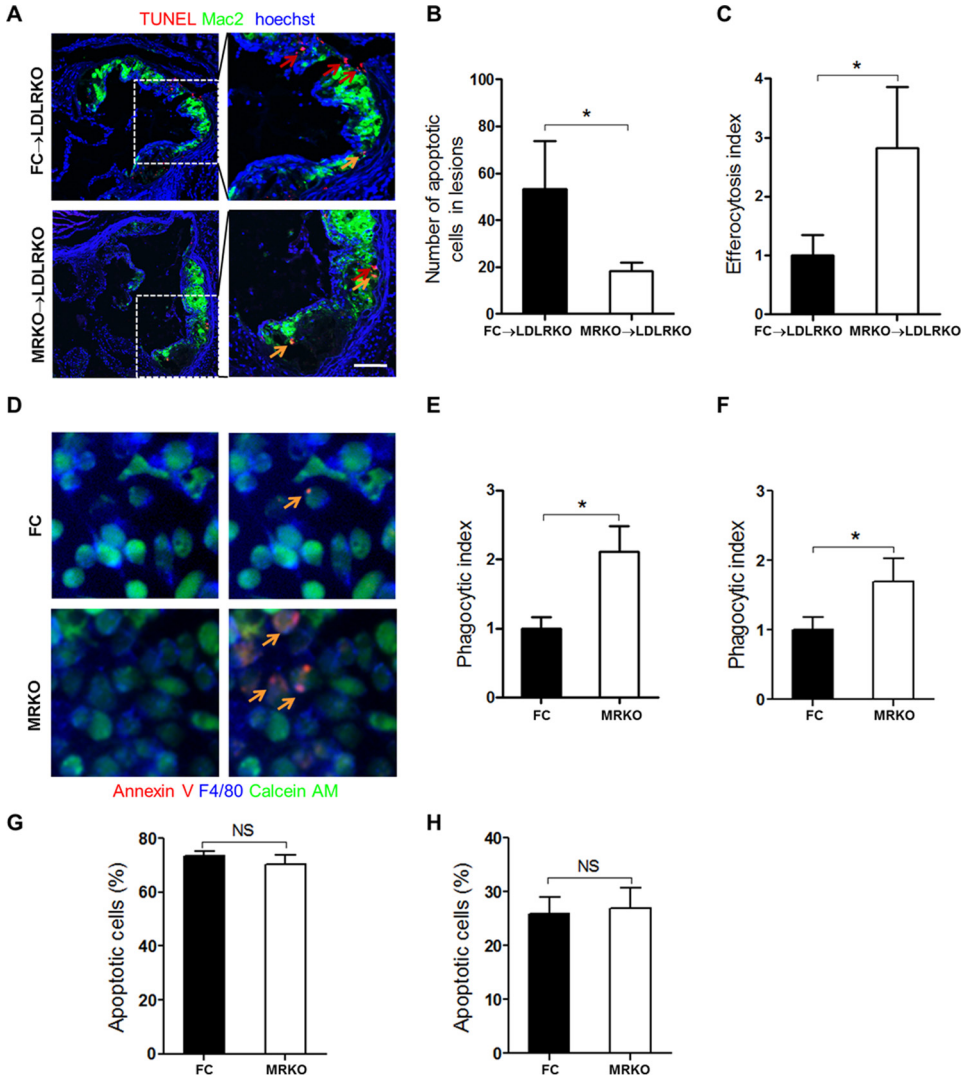

FIGURE 9. **Myeloid MR deficiency increases efferocytosis of macrophages.** *A*, representative immunofluorescence staining of macrophage efferocytosis in aortic sinus from FC → LDLRKO mice and MRKO → LDLRKO mice. Macrophages or foam cells were stained with mac2 (*green*) and apoptotic cells were stained with TUNEL (*red*). *Red arrows* indicate free apoptotic cells. *Yellow arrows* indicate macrophage-associated apoptotic cells. *B*, quantification of apoptotic cells in the lesions ($n = 5$–7). *C*, quantification of efferocytosis index in the lesions. The efferocytosis index is the macrophage-associated apoptotic cells/free apoptotic cells ($n = 5$–7). *D*, representative immunofluorescence staining of apoptotic macrophages phagocytized by BMDMs from FC or MRKO mice. Viable cells were labeled with calcein AM (*green*), macrophages were labeled with F4/80 (*blue*), and apoptotic cells were labeled with Alexa Fluor 594-annexin V (*red*). *Yellow arrows* indicate macrophages that have phagocytized apoptotic cells. *E*, quantification of phagocytic index of BMDMs from FC and MRKO mice ($n = 3$). *F*, quantification of phagocytic index of peritoneal macrophages from FC and MRKO mice ($n = 5$). *G*, the ratio of apoptotic peritoneal macrophages incubated with 7KC ($n = 4$). *H*, the ratio of apoptotic BMDMs incubated with 7KC ($n = 4$). *NS*, not significant. *, $p < 0.05$.

TABLE 1
Survival rates of irradiated mice with or without bone marrow transplantation

	FC → LDLRKO mice	MRKO → LDLRKO mice
Survival rates without BMT (%)[a]	0	0
Survival rates with BMT (%)	87.50	94.44

[a] BMT, bone marrow transplantation.

cholesterol (7KC) for 19 h and labeled with Alexa Fluor 594-annexin V (*red*; Invitrogen). Viable cells were labeled with calcein AM (*green*; BD Biosciences). Macrophages (phagocytes) were stained with F4/80 (*blue*; Abcam). The apoptotic macrophages and phagocytic macrophages were mixed at a ratio of 1:1 and incubated at 37 °C for 1 h. Macrophage phagocytic index was determined as the ratio of macrophages harboring apoptotic cells to total number of macrophages (41, 42).

Measurements of Oxidative Status—For macrophage-mediated LDL oxidation, peritoneal macrophages were incubated with LDL (100 μg/ml) in phenol-free DMEM supplemented with 2 μM $CuSO_4$. After 6 h, the extent of LDL oxidation was measured by thiobarbituric acid reactive substance assay, and the results were expressed as nmolmalondialyde/mg LDL (21). For cellular lipid peroxidation, macrophages were incubated with dichlorofluorescein diacetete (2.5×10^{-5} mol/liter per 2×10^6 cells) at 37 °C for 30 min. Mean fluorescence intensity was assayed with flow cytometry (FACSAria; BD Biosciences) (43). For cellular superoxide anion production, macrophages were incubated with Krebs-Henseleit/HEPES buffer and 10 μmol/liter dark-adapted lucigenin for 10 min. After the addition of NADPH (100 μmol/liter), chemiluminescence was recorded every 2 min by spectrophotometry (43).

Statistical Analysis—The data were reported as the means ± S.E. GraphPad Prism 5.0 was used for data analysis (GraphPad Software). Student's *t* test was used for pair-wise comparisons, and two-way ANOVA was used for multiple comparisons. The incidence of aortic aneurysm was analyzed by SPSS 17.

Author Contributions—S.-Z. D. designed and coordinated the study and wrote the paper. Z.-X. S. designed and performed experiments, analyzed data, and wrote the paper. X.-Q. C., X.-N. S., J.-Y. S., W.-C. Z., X.-J. Z., Y.-Y. Z., H.-J. S., J.-W. Z., and C. L. performed experiments. J. W. and X. L. designed and coordinated the study.

References

1. Mendis, S., Puska, P., and Norrving, B. (2011) *Global Atlas on Cardiovascular Disease Prevention and Control*, World Health Organization, World Heart Federation and World Stroke Organization
2. Libby, P., Bornfeldt, K. E., and Tall, A. R. (2016) Atherosclerosis: successes, surprises, and future challenges. *Circ. Res.* **118,** 531–534
3. Tabas, I., and Bornfeldt, K. E. (2016) Macrophage phenotype and function in different stages of atherosclerosis. *Circ. Res.* **118,** 653–667
4. Moore, K. J., and Tabas, I. (2011) Macrophages in the pathogenesis of atherosclerosis. *Cell* **145,** 341–355
5. Moore, K. J., Sheedy, F. J., and Fisher, E. A. (2013) Macrophages in atherosclerosis: a dynamic balance. *Nat. Rev. Immunol.* **13,** 709–721
6. Lother, A., Moser, M., Bode, C., Feldman, R. D., and Hein, L. (2015) Mineralocorticoids in the heart and vasculature: new insights for old hormones. *Annu. Rev. Pharmacol. Toxicol.* **55,** 289–312
7. McCurley, A., and Jaffe, I. Z. (2012) Mineralocorticoid receptors in vascular function and disease. *Mol. Cell. Endocrinol.* **350,** 256–265
8. Ferrario, C. M., and Schiffrin, E. L. (2015) Role of mineralocorticoid receptor antagonists in cardiovascular disease. *Circ. Res.* **116,** 206–213
9. Pitt, B., Zannad, F., Remme, W. J., Cody, R., Castaigne, A., Perez, A., Palensky, J., and Wittes, J. (1999) The effect of spironolactone on morbidity and mortality in patients with severe heart failure: Randomized Aldactone Evaluation Study Investigators. *N. Engl. J. Med.* **341,** 709–717
10. Pitt, B., Remme, W., Zannad, F., Neaton, J., Martinez, F., Roniker, B., Bittman, R., Hurley, S., Kleiman, J., and Gatlin, M. (2003) Eplerenone, a selective aldosterone blocker, in patients with left ventricular dysfunction after myocardial infarction. *N. Engl. J. Med.* **348,** 1309–1321
11. Zannad, F., McMurray, J. J., Krum, H., van Veldhuisen, D. J., Swedberg, K., Shi, H., Vincent, J., Pocock, S. J., and Pitt, B. (2011) Eplerenone in patients with systolic heart failure and mild symptoms. *N. Engl. J. Med.* **364,** 11–21
12. Moss, M. E., and Jaffe, I. Z. (2015) Mineralocorticoid receptors in the pathophysiology of vascular inflammation and atherosclerosis. *Front. Endocrinol.* (*Lausanne*) **6,** 153
13. Rickard, A. J., Morgan, J., Tesch, G., Funder, J. W., Fuller, P. J., and Young, M. J. (2009) Deletion of mineralocorticoid receptors from macrophages protects against deoxycorticosterone/salt-induced cardiac fibrosis and increased blood pressure. *Hypertension* **54,** 537–543
14. Usher, M. G., Duan, S. Z., Ivaschenko, C. Y., Frieler, R. A., Berger, S., Schütz, G., Lumeng, C. N., and Mortensen, R. M. (2010) Myeloid mineralocorticoid receptor controls macrophage polarization and cardiovascular hypertrophy and remodeling in mice. *J. Clin. Invest.* **120,** 3350–3364
15. Bienvenu, L. A., Morgan, J., Rickard, A. J., Tesch, G. H., Cranston, G. A., Fletcher, E. K., Delbridge, L. M., and Young, M. J. (2012) Macrophage mineralocorticoid receptor signaling plays a key role in aldosterone-independent cardiac fibrosis. *Endocrinology* **153,** 3416–3425
16. Li, C., Zhang, Y. Y., Frieler, R. A., Zheng, X. J., Zhang, W. C., Sun, X. N., Yang, Q. Z., Ma, S. M., Huang, B., Berger, S., Wang, W., Wu, Y., Yu, Y., Duan, S. Z., and Mortensen, R. M. (2014) Myeloid mineralocorticoid receptor deficiency inhibits aortic constriction-induced cardiac hypertrophy in mice. *PLoS One* **9,** e110950
17. Sun, J. Y., Li, C., Shen, Z. X., Zhang, W. C., Ai, T. J., Du, L. J., Zhang, Y. Y., Yao, G. F., Liu, Y., Sun, S., Naray-Fejes-Toth, A., Fejes-Toth, G., Peng, Y., Chen, M., Liu, X., *et al.* (2016) Mineralocorticoid receptor deficiency in macrophages inhibits neointimal hyperplasia and suppresses macrophage inflammation through SGK1-AP1/NF-$\kappa\beta$ pathways. *Arterioscler. Thromb. Vasc. Biol.* **36,** 874–885
18. Kojima, Y., Downing, K., Kundu, R., Miller, C., Dewey, F., Lancero, H., Raaz, U., Perisic, L., Hedin, U., Schadt, E., Maegdefessel, L., Quertermous, T., and Leeper, N. J. (2014) Cyclin-dependent kinase inhibitor 2B regulates efferocytosis and atherosclerosis. *J. Clin. Invest.* **124,** 1083–1097
19. Raz-Pasteur, A., Gamliel-Lazarovich, A., Gantman, A., Coleman, R., and Keidar, S. (2014) Mineralocorticoid receptor blockade inhibits accelerated atherosclerosis induced by a low sodium diet in apolipoprotein E-deficient mice. *J. Renin Angiotensin Aldosterone Syst.* **15,** 228–235
20. Takai, S., Jin, D., Muramatsu, M., Kirimura, K., Sakonjo, H., and Miyazaki, M. (2005) Eplerenone inhibits atherosclerosis in nonhuman primates. *Hypertension* **46,** 1135–1139
21. Keidar, S., Hayek, T., Kaplan, M., Pavlotzky, E., Hamoud, S., Coleman, R., and Aviram, M. (2003) Effect of eplerenone, a selective aldosterone blocker, on blood pressure, serum and macrophage oxidative stress, and atherosclerosis in apolipoprotein E-deficient mice. *J. Cardiovasc. Pharmacol.* **41,** 955–963
22. Rajagopalan, S., Duquaine, D., King, S., Pitt, B., and Patel, P. (2002) Mineralocorticoid receptor antagonism in experimental atherosclerosis. *Circulation* **105,** 2212–2216
23. Fredman, G., Kamaly, N., Spolitu, S., Milton, J., Ghorpade, D., Chiasson, R., Kuriakose, G., Perretti, M., Farokhzad, O., and Tabas, I. (2015) Targeted nanoparticles containing the proresolving peptide Ac2–26 protect against advanced atherosclerosis in hypercholesterolemic mice. *Sci. Transl. Med.* **7,** 275ra20
24. Lewis, D. R., Petersen, L. K., York, A. W., Zablocki, K. R., Joseph, L. B., Kholodovych, V., Prud'homme, R. K., Uhrich, K. E., and Moghe, P. V. (2015) Sugar-based amphiphilic nanoparticles arrest atherosclerosis *in vivo*. *Proc. Natl. Acad. Sci. U.S.A.* **112,** 2693–2698
25. Leuschner, F., Dutta, P., Gorbatov, R., Novobrantseva, T. I., Donahoe, J. S., Courties, G., Lee, K. M., Kim, J. I., Markmann, J. F., Marinelli, B., Panizzi, P., Lee, W. W., Iwamoto, Y., Milstein, S., Epstein-Barash, H., *et al.* (2011) Therapeutic siRNA silencing in inflammatory monocytes in mice. *Nat. Biotechnol.* **29,** 1005–1010
26. Duivenvoorden, R., Tang, J., Cormode, D. P., Mieszawska, A. J., Izquierdo-Garcia, D., Ozcan, C., Otten, M. J., Zaidi, N., Lobatto, M. E., van Rijs, S. M., Priem, B., Kuan, E. L., Martel, C., Hewing, B., Sager, H., *et al.* (2014) A statin-loaded reconstituted high-density lipoprotein nanoparticle inhibits atherosclerotic plaque inflammation. *Nat. Commun.* **5,** 3065
27. Finn, A. V., Nakano, M., Narula, J., Kolodgie, F. D., and Virmani, R. (2010) Concept of vulnerable/unstable plaque. *Arterioscler. Thromb. Vasc. Biol.* **30,** 1282–1292
28. Keidar, S., Gamliel-Lazarovich, A., Kaplan, M., Pavlotzky, E., Hamoud, S., Hayek, T., Karry, R., and Abassi, Z. (2005) Mineralocorticoid receptor blocker increases angiotensin-converting enzyme 2 activity in congestive heart failure patients. *Circ. Res.* **97,** 946–953
29. Li, A. C., Binder, C. J., Gutierrez, A., Brown, K. K., Plotkin, C. R., Pattison, J. W., Valledor, A. F., Davis, R. A., Willson, T. M., Witztum, J. L., Palinski, W., and Glass, C. K. (2004) Differential inhibition of macrophage foam-cell formation and atherosclerosis in mice by PPARα, β/δ, and γ. *J. Clin. Invest.* **114,** 1564–1576
30. Chawla, A., Boisvert, W. A., Lee, C.-H., Laffitte, B. A., Barak, Y., Joseph, S. B., Liao, D., Nagy, L., Edwards, P. A., Curtiss, L. K., Evans, R. M., and Tontonoz, P. (2001) A PPARγ-LXR-ABCA1 pathway in macrophages is involved in cholesterol efflux and atherogenesis. *Mol. Cell* **7,** 161–171
31. Chinetti, G., Lestavel, S., Bocher, V., Remaley, A. T., Neve, B., Torra, I. P., Teissier, E., Minnich, A., Jaye, M., Duverger, N., Brewer, H. B., Fruchart, J.-C., Clavey, V., and Staels, B. (2001) PPAR-α and PPAR-γ activators induce cholesterol removal from human macrophage foam cells through stimulation of the ABCA1 pathway. *Nat. Med.* **7,** 53–58
32. Van Vré, E. A., Ait-Oufella, H., Tedgui, A., and Mallat, Z. (2012) Apoptotic cell death and efferocytosis in atherosclerosis. *Arterioscler. Thromb. Vasc. Biol.* **32,** 887–893
33. Hanna, R. N., Shaked, I., Hubbeling, H. G., Punt, J. A., Wu, R., Herrley, E., Zaugg, C., Pei, H., Geissmann, F., Ley, K., and Hedrick, C. C. (2012) NR4A1

(Nur77) deletion polarizes macrophages toward an inflammatory phenotype and increases atherosclerosis. *Circ. Res.* **110,** 416–427
34. Daugherty, A., Manning, M. W., and Cassis, L. A. (2000) Angiotensin II promotes atherosclerotic lesions and aneurysms in apolipoprotein E-deficient mice. *J. Clin. Invest.* **105,** 1605–1612
35. Ding, L., Biswas, S., Morton, R. E., Smith, J. D., Hay, N., Byzova, T. V., Febbraio, M., and Podrez, E. A. (2012) Akt3 deficiency in macrophages promotes foam cell formation and atherosclerosis in mice. *Cell Metab.* **15,** 861–872
36. Ducharme, A., Frantz, S., Aikawa, M., Rabkin, E., Lindsey, M., Rohde, L. E., Schoen, F. J., Kelly, R. A., Werb, Z., Libby, P., and Lee, R. T. (2000) Targeted deletion of matrix metalloproteinase-9 attenuates left ventricular enlargement and collagen accumulation after experimental myocardial infarction. *J. Clin. Invest.* **106,** 55–62
37. Macritchie, N., Grassia, G., Sabir, S. R., Maddaluno, M., Welsh, P., Sattar, N., Ialenti, A., Kurowska-Stolarska, M., McInnes, I. B., Brewer, J. M., Garside, P., and Maffia, P. (2012) Plasmacytoid dendritic cells play a key role in promoting atherosclerosis in apolipoprotein E-deficient mice. *Arterioscler. Thromb. Vasc. Biol.* **32,** 2569–2579
38. Weischenfeldt, J., and Porse, B. (2008) Bone marrow-derived macrophages (BMM): isolation and applications. *Cold Spring Harbor Protocols* **2008,** pdb.prot5080
39. Zhang, X., Goncalves, R., and Mosser, D. M. (2008) The isolation and characterization of murine macrophages. *Curr. Protoc. Immunol.* Chapter 14, Unit 14.11
40. Rousselle, A., Qadri, F., Leukel, L., Yilmaz, R., Fontaine, J.-F., Sihn, G., Bader, M., Ahluwalia, A., and Duchene, J. (2013) CXCL5 limits macrophage foam cell formation in atherosclerosis. *J. Clin. Invest.* **123,** 1343–1347
41. Thorp, E., Cui, D., Schrijvers, D. M., Kuriakose, G., and Tabas, I. (2008) Mertk receptor mutation reduces efferocytosis efficiency and promotes apoptotic cell accumulation and plaque necrosis in atherosclerotic lesions of Apoe$^{-/-}$ mice. *Arterioscler. Thromb. Vasc. Biol.* **28,** 1421–1428
42. Heo, K. S., Cushman, H. J., Akaike, M., Woo, C. H., Wang, X., Qiu, X., Fujiwara, K., and Abe, J. (2014) ERK5 Activation in macrophages promotes efferocytosis and inhibits atherosclerosis. *Circulation* **130,** 180–191
43. Keidar, S., Kaplan, M., Pavlotzky, E., Coleman, R., Hayek, T., Hamoud, S., and Aviram, M. (2004) Aldosterone administration to mice stimulates macrophage NADPH oxidase and increases atherosclerosis development: a possible role for angiotensin-converting enzyme and the receptors for angiotensin II and aldosterone. *Circulation* **109,** 2213–2220